ТРАНСПОРТНЫЕ СИСТЕМЫ
2.9.1 – Транспортные и транспортно-технологические системы страны, ее регионов и городов, организация производства на транспорте;
2.9.4. – Управление процессами перевозок;
2.9.6 – Аэронавигация и эксплуатация авиационной техники;
2.9.8 – Интеллектуальные транспортные системы

УДК 621.396.959.3
DOI: 10.26467/2079-0619-2026-29-1-23-37

The use of onboard decimeter-band radar stations for humanitarian demining

O.V. Vasiliev[1], P.S. Gorshkov[1], S.A. Zyabkin[1], I.P. Shepet'[2]
[1]NaukaSoft Scientific and Production Association, Moscow, Russia
[2]Technological Institute of Service (branch of DSTU), Stavropol, Russia

Abstract: Humanitarian demining is a pressing issue today. This paper examines various technical means used in engineer reconnaissance to detect mines and substantiates the need for radar support for humanitarian engineer reconnaissance. An airborne engineer reconnaissance radar system based on a side-looking P-band radar, intended for deployment on unmanned aerial vehicles, is proposed as the main information link. The physical principles of radar image formation using aperture synthesis are described. The application of the radar relief function in describing the radio-reflective properties of a surface and the use of the superposition principle in radar signal processing are demonstrated. The main mathematical expressions used in calculating radar images of a surface using the aperture synthesis method are presented, consisting of the application of correlation signal processing independently by the coordinates of the ground and slant ranges. The features of using the decimeter range of electromagnetic waves in constructing radar images for the purpose of detecting mines on various underlying surfaces are analyzed and a comparison with the centimeter range is made. The demonstrated advantages include a significant increase in the contrast of metal objects against the background of reflection from the underlying surface and an increase in the penetration depth into the underlying surface. Disadvantages are also identified, including increased requirements for the stability of the flight of the carrier, the need to increase the size of the aperture to achieve comparable detail and take into account the migration of range channels. The software architecture is demonstrated, comprising an onboard unit for acquiring radar images and a graphical interface for a ground-based automated operator-decipherer workstation for solving the problem of mine detection during humanitarian demining. A sample system and the results of its testing on various carriers, including quadcopter and vertical takeoff and landing (VTOL) unmanned aerial vehicles, are presented.

Key words: humanitarian demining, engineer reconnaissance, airborne side-looking P-band synthetic aperture radar, information support for humanitarian demining, unmanned aerial vehicle.

For citation: Vasiliev, O.V., Gorshkov, P.S., Zyabkin, S.A., Shepet', I.P. (2026). The use of onboard decimeter-band radar stations for humanitarian demining. Civil Aviation High Technologies, vol. 29, no. 1, pp. 23–37. DOI: 10.26467/2079-0619-2026-29-1-23-37

Применение бортовых радиолокационных станций дециметрового диапазона при гуманитарном разминировании

О.В. Васильев[1], П.С. Горшков[1], С.А. Зябкин[1], И.П. Шепеть[2]
[1]ООО «НПО НаукаСофт», г. Москва, Россия
[2]Технологический институт сервиса (филиал ДГТУ), г. Ставрополь, Россия

Аннотация: Проблема гуманитарного разминирования на текущий момент чрезвычайно актуальна. В работе рассмотрены различные технические средства, применяемые в инженерной разведке для решения задачи обнаружения мин, и обоснована необходимость радиолокационного обеспечения гуманитарной инженерной разведки. В качестве

основного информационного звена предложен авиационный радиолокационный комплекс инженерной разведки на базе радиолокационной станции бокового обзора Р-диапазона, предназначенный для размещения на беспилотных летательных аппаратах. Описаны физические принципы формирования радиолокационного изображения методом синтеза апертуры. Показано применение функции радиолокационного рельефа при описании радиоотражающих свойств поверхности и использование принципа суперпозиций при обработке радиолокационного сигнала. Представлены основные математические выражения, применяемые при расчете радиолокационных изображений поверхности методом синтеза апертуры, заключающиеся в применении корреляционной обработки сигнала независимо по координатам путевой и наклонной дальностей. Проанализированы особенности использования дециметрового диапазона электромагнитных волн при построении радиолокационных изображений в интересах обнаружения мин на различных подстилающих поверхностях, и проведено сравнение с сантиметровым диапазоном. В качестве преимуществ продемонстрировано значительное увеличение контраста металлических объектов на фоне отражения от подстилающей поверхности и возрастание глубины проникновения в подстилающую поверхность. Также сформулированы недостатки, включающие в себя повышенные требования к стабильности полета носителя, необходимость увеличения размера апертуры для достижения сопоставимой детальности и учета миграции каналов дальности. Продемонстрирована структура программного обеспечения, содержащего бортовую часть для получения радиолокационных изображений и графический интерфейс наземного автоматизированного рабочего места оператора-дешифровщика для решения задачи поиска мин при гуманитарном разминировании. Показан образец комплекса и результаты его испытаний на различных носителях, включающих беспилотные летательные аппараты классов «квадрокоптер» и вертикального взлета и посадки (VTOL).

Ключевые слова: гуманитарное разминирование, инженерная разведка, бортовая радиолокационная станция с синтезированной апертурой бокового обзора Р-диапазона, информационное обеспечение гуманитарного разминирования, беспилотный летательный аппарат.

Для цитирования: Васильев О.В. Применение бортовых радиолокационных станций дециметрового диапазона при гуманитарном разминировании / О.В. Васильев, П.С. Горшков, С.А. Зябкин, И.П. Шепеть // Научный вестник МГТУ ГА. 2026. Т. 29, № 1. С. 23–37. DOI: 10.26467/2079-0619-2026-29-1-23-37

Introduction

Humanitarian demining is an activity carried out outside combat zones in cooperation with local governments (territorial administrations) that leads to the elimination of hazards (risks) associated with explosive ordnance (EO), including a comprehensive survey of the area and facilities for the presence of EO, mapping, searching and disposal of EO, and preparing documentation after demining.[1]

A characteristic feature of modern warfare is the widespread and massive mining of vast territories. Moreover, the vast majority of mines and EO are not equipped with self-destruct mechanisms. This makes their search and clearance mandatory. Current mine search methods using a deminer do not ensure mine clearance in a short time, and the use of unmanned mine clearers is impossible for clearing anti-tank mines.

In this case, conducting engineer reconnaissance using technical means for humanitarian demining is a pressing issue. At the same time, a whole range of devices is proposed as technical means, the operation of which is based on a wide range of physical principles.

This article substantiates the use of a side-looking synthetic aperture radar in the decimeter band for searching for antitank mines over large areas. The features of using the decimeter band, as well as its advantages and disadvantages for conducting engineer reconnaissance, are analyzed. The results of flight experiments on searching for and detecting mines and their simulators on various soils using radars mounted on various platforms are presented. A conclusion is drawn regarding the high effectiveness of this type of radar for conducting engineer reconnaissance for humanitarian demining.

Technical means used in engineer reconnaissance

Traditionally, the primary tools for explosive ordnance detection and mine clearance are: a probe

[1] Practical activities (humanitarian demining). *Ministry of Defense of the Russian Federation*. Available at: https://mil.ru/mpc/activities/practical.htm (accessed: 21.04.2025).

and mine detectors. Specially trained dogs can be used to reduce the risk to the lives of the deminers [1].

Attempts to reduce risks and automate the mine clearance process are underway in many countries, but so far without significant results.

However, over the past few years, the use of unmanned aerial vehicles (UAVs) in engineer reconnaissance has reached a large scale [2]. Many government and non-profit agencies involved in humanitarian demining are implementing UAVs into their standard procedures. In addition to collecting aerial photographs of potentially hazardous areas to create orthophoto maps, UAVs already prioritize demining zones and, in some cases, detect mines.

At the current stage of remote mine reconnaissance, the following sensors can be used as UAV payloads: visible-band video cameras (TV cameras), infrared cameras (IR cameras), scanning laser locators (SLRs), and magnetometric sensors (MS). All of these differ in both their application features and their information capabilities for detecting and classifying explosive ordnance [3].

TV cameras are characterized by high speed and detailed viewing of the surface being surveyed. However, image quality is significantly affected by meteorological and daily conditions. Furthermore, at least 60,000 images are required to cover 1 square kilometer with acceptable resolution.

One of the promising approaches to mine detection is the use of infrared cameras. This method is based on the differences in thermal radiation between the underlying soil and a small area where a mine is located or buried. However, experimental studies have revealed a high rate of false alarms caused by anomalies in soil moisture or density.

A laser locator is useful for detecting craters indicating ground disturbances, but it cannot detect buried objects.

Magnetometers are currently the best tools for detecting buried metal objects. However, the magnetic signal weakens as the magnetometer moves away from the ground, necessitating the use of UAVs at low altitudes.

One of the most promising areas for increasing the efficiency of mine reconnaissance is the use of side-looking synthetic aperture radar (SAR) as a target load for UAVs [4].

Physical principles of radar image formation in SAR

The radar relief function (RRF) is used as a mathematical model of the reflective properties of the observed surface. It defines the complex envelope of the electromagnetic field $\dot{e}$, scattered from the underlying surface and is numerically dependent on the local surface reflectivity and signal parameters according to the following formula [5]:

$$\dot{e}(r,x) = e(r,x) \cdot \exp\{j\psi(r,x)\}, \qquad (1)$$

where x and $r = \sqrt{y^2 + H^2}$ are coordinates along the path and slant ranges, respectively; $e(r,x)$ and $\psi(r,x)$ are the amplitude and phase characteristics of the scattered electromagnetic field. Based on [5], if we do not take into account changes in the reflective properties of the surface in the observation interval $X_н = r_0\theta_A$, where θ_A is the antenna radiation pattern (RP) width, we can limit ourselves to the dependence on spatial coordinates only. The formation of the synthetic aperture of the antenna in the side-looking SAR is shown in Figure 1.

In Figure 1, the variable $T_з$ characterizes the pulse recurrence interval, $V_п$ is the carrier's flight speed. It is known that the process of generating and processing a radar signal obeys the principle of superposition due to the linearity of operations [6]. This means that the signal from each elementary reflector on the observed terrain can be processed independently, and reflections from a complex spatially distributed object can be represented as the sum of signals from several point targets on its surface.

The signal $\dot{s}(\tau, n)$ in a side-looking SAR from the i-th point target at the receiver output is continuous over slant range $\tau = 2\,r/c$ and discrete over ground range $nT_з$ (n = 0, 1, 2, …), and also independent over these coordinates [7]:

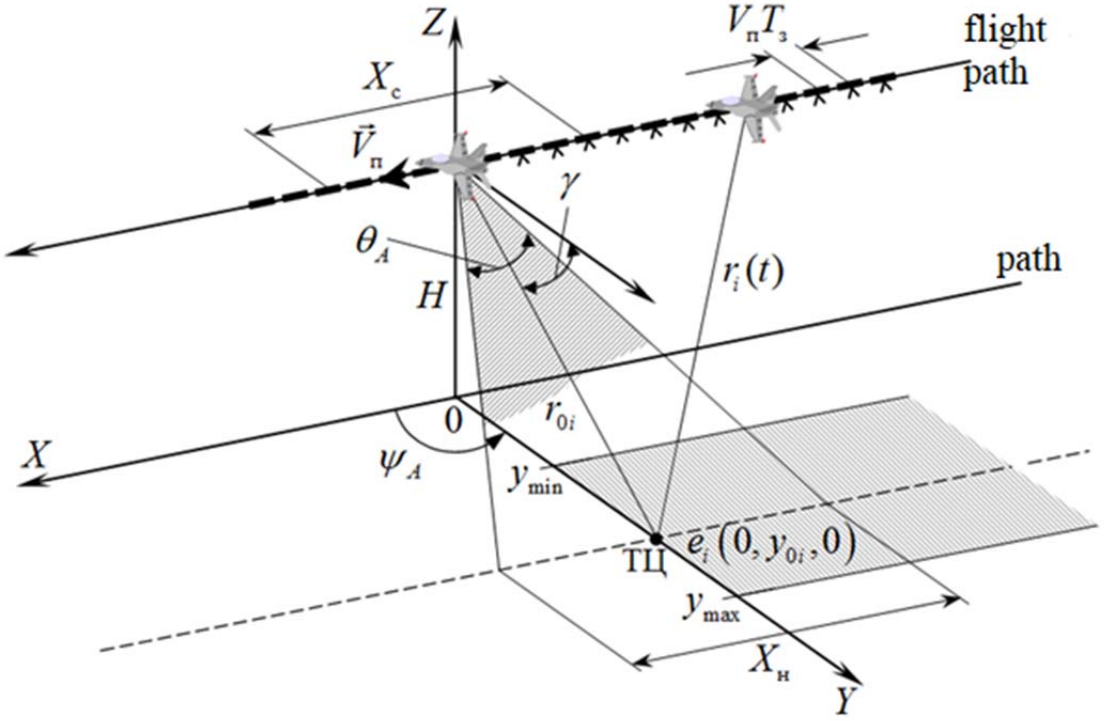

Fig. 1. Formation of the synthetic aperture of the antenna at $\Psi_A = \pi/2$

$$\dot{s}_i(\tau, n) = \dot{s}_i(\tau, nT_з) = \eta_i U_i(\tau - \tau_i) \cdot G(\tau, nT_з) \times \\ \times exp\{j \cdot [\psi(\tau - \tau_i) - \alpha(nT_з)^2 + \varphi_i]\}, \quad (2)$$

where τ_i is the time delay of the signal from the *i*-th point target along the slant range during the probing period; $\alpha = 2\pi V_п/\lambda r_{0i}$; $\psi(\tau)$ is the function describing the phase modulation law of the probing signals; $U_i(\tau)$ is the function describing the amplitude envelope of the signal from the *i*-th elementary reflector; $G(\tau, nT_з)$ is the signal envelope along the path coordinate x.

When using a probing chirp pulse, the signal from the *i*-th elementary reflector, located at a distance of r_i, $m\Delta r \le r_i \le (m+1)\Delta r$, is determined by the formula

$$\dot{s}_i(m, n) = \eta_i U_i[(m - m_i)\Delta r] G(m\Delta r, (n - n_i)\Delta x) \times \\ \times exp\left\{-j \cdot \left[\frac{2\alpha_r}{c^2}\left((m - m_i)\Delta r\right)^2 + \frac{2\pi}{m\Delta r\lambda}\left((n - n_i)\Delta x\right)^2 + \varphi_i\right]\right\}, \quad (3)$$

$\Delta r = \delta r/k_r$ and $\Delta x = V_п T_з$ are the sampling intervals for coordinates x and r; $a_r = 2\Delta\omega/\tau_u$ is the chirp step slope; $\Delta\omega = 2\pi\Delta f$ is the frequency deviation.

The signal reflected from the earth's surface and complex objects $\dot{\xi}(\tau, n)$, is a superposition of noise and responses from all elementary reflectors within the radiation pattern:

$$\dot{\xi}(\tau, n) = \sum_i \dot{s}_i(\tau, n) + \dot{n}(\tau, n), \quad (4)$$

where $\dot{n}(\tau, n)$ is complex white noise.

As mentioned earlier, the signal cross-sections $\dot{s}_i(m, n)$ along the ground (when fixing the coordinate m) and slant (when fixing n) ranges are independent in the absence of signal migration from point targets in the slant range band during the synthesis interval, and the signal

Table 1

Approximate RCS values for typical surfaces

Terrain type	Specific radar cross-section σ_0, dB		
	$\lambda = 3.0\ cm$		$\lambda = 70.0\ cm$
	HH	VV	HH and VV
Sea, 2-point waves	−38	−28	−45
Sea, 6-point waves	−30	−25	−45
Runway	−32	−24	−58
Steppe, winter, snow	−17	−17	−55
Steppe, summer, grass	−15	−15	−53
Desert, rocks, sand	−15	−17	−40
Forest	−14	−15	−30

itself $\dot{s}_i(m,n)$ is separable by coordinates m and n [5]. Therefore, algorithms for this processing can be developed independently by coordinates m and n. The goal of the processing is to compress signals from each element of the observed surface based on the existing signal spectrum expansion in the cross-sections by coordinates r and x, thereby ensuring high resolution in the ground and slant range coordinates.

It is known that radar signals with an extended baseline are compressed in duration using *correlation processing* [8]. This uses a reference function matched to the signal from an elementary reflector. This function, like the signal, is separated by coordinates x and r: $\dot{h}_0(m,n) = \dot{h}_{0r}(m) \cdot \dot{h}_{0x}(n) = \dot{s}_i^*(m,n)$ (the * symbol denotes complex conjugation):

$$\dot{e}(m,n) = \left|\sum_{k=0}^{N-1}\sum_{l=0}^{M-1}\dot{\xi}(l-m,k-n)\dot{h}_0(l,k)\right| = \\ = \left|\sum_{l=0}^{N-1}\left\{\sum_{l=0}^{M-1}\dot{\xi}(l-m,k-n)\dot{h}_{0r}(l)\right\}\cdot\dot{h}_{0x}(k)\right|, \quad (5)$$

where $m = 0,1,\ldots,M_r-1; n = 0,1,\ldots,N_x$; M and N and is the number of reference function samples along the slant $\dot{h}_{0r}(m)$ and path $\dot{h}_{0x}(n)$ distances.

The reference function $\dot{h}(m,n)$, phase-matched with the signal from the point reflector over the synthesis interval $X_c = N_c V_{\text{п}} T_{\text{з}} = N_c \Delta x$, is described by the formula

$$\dot{h}(m,n) = H(m,n)\cdot exp\left\{j\frac{2\pi}{m\Delta r\lambda}(n\Delta x)^2\right\}, \quad (6)$$

where $H(m,n)$ is the pulse response envelope of the digital filter, specified on the integrated circuit: $n = 0,1,2,\ldots,N_c-1$.

Features of P-band radar images

Target detection efficiency is determined by the signal-to-background ratio q, which is equal to the ratio of the target's RCS $\sigma_{\text{ц}}$ to the background RCS $\sigma_{\text{ф}}$ in a resolution element:

$$q = \frac{\sigma_{\text{ц}}}{\sigma_{\text{ф}}} = \frac{\sigma_{\text{ц}}}{\sigma_0 \delta r \delta l}, \quad (7)$$

where δr and δl the linear resolutions for range and angle, respectively, σ_0 is the specific RCS of the surface.

Approximate values of specific RCS for various underlying surfaces for the *X* (3 cm) and *P* (70 cm) bands at a 20° radiation incidence angle are presented in Table 1 [9]. The values are shown for various polarizations, where HH is the horizontal polarization for reception and transmission, and VV is the vertical polarization for reception and transmission.

As the table shows, the transition from the centimeter to the decimeter range is marked by an abrupt change, primarily in the reflectivity of

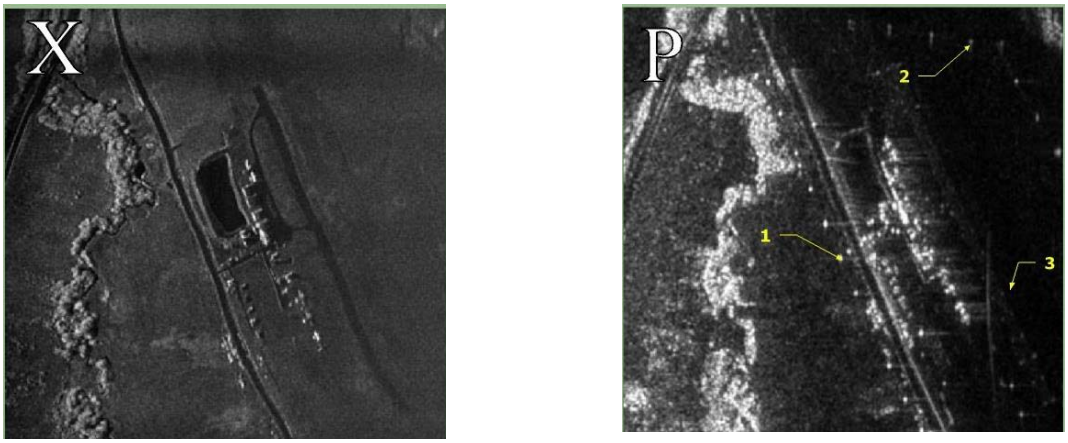

a b

Fig. 2. Radar image of a section with a road, a pond, and a small aircraft airfield:
a – in the X-band; *b* – in the P-band

the underlying surface. Thus, in the range λ = 70 cm the average specific RCS σ_0 decreases by 20…30 dB, leading to an increase in the radar contrast of objects relative to the background.

It is also clear from expression (7) that maximum detection efficiency is achieved when the resolution element size of the side-looking SAR $\delta r, \delta l$ corresponds to the linear dimensions of the object (target) on the surface in the y and x coordinates, respectively. High resolution in slant range (y coordinate) is achieved by using broadband signals, and in the direction of ground speed (x coordinate) by using long intervals of trajectory signal accumulation.

Figure 2 shows radar images obtained using a dual-band integrated airborne side-looking SAR [10, 11]. The flight altitude of the carrier (Antonov-2 aircraft) is 800 m, the range to the center of the radar image is 2000 m. In Figure 2, *a* on the X-band radar image (wavelength λ = 3 cm) an airfield for small aircraft with infrastructure, a road and a pond are observed. In Figure 2, *b* on the P-band radar images (wavelength λ = 70 cm) lampposts and a ditch along the road, individual buildings, technical equipment, aircraft (marked with the corresponding markers 1–3 in Figure 2, *b* are clearly visible.

The specific features of P-band use, most of which are evident in Figure 2, include:

- the contrast of metallic objects significantly increases (by 20–30 dB) against reflections from the underlying surface;
- resonance phenomena begin to play a role;
- greater penetration depth into the underlying surface is ensured compared to the centimeter band.

At the same time, the use of P-band side-looking SAR poses objective difficulties in radar image formation.

Firstly, the relatively low carrier frequency precludes the use of signals with a spectral width greater than 100 MHz (20–25% of the carrier). In this case, the maximum slant range resolution δr is 1.5 m.

Secondly, a longer wavelength for achieving high azimuth resolution δl (commensurate with δr) requires a larger synthesized aperture size, which means longer trajectory signal accumulation intervals at the same carrier flight speeds [12]. The dependences of the aperture size X_c on the distance to the target r_o for different azimuth resolutions for two frequency bands are shown in Figure 3.

Thus, for δl = 1.5 m, r_0 = 1000 m, λ = 0.7 m, the synthesis interval will be more than 200 m. To achieve the same radar image detail in the X-band, the synthesis interval does not exceed 9 m.

Thirdly, the condition for a linearly matched processing range of the accumulated trajectory signal is satisfied in the absence of migration of

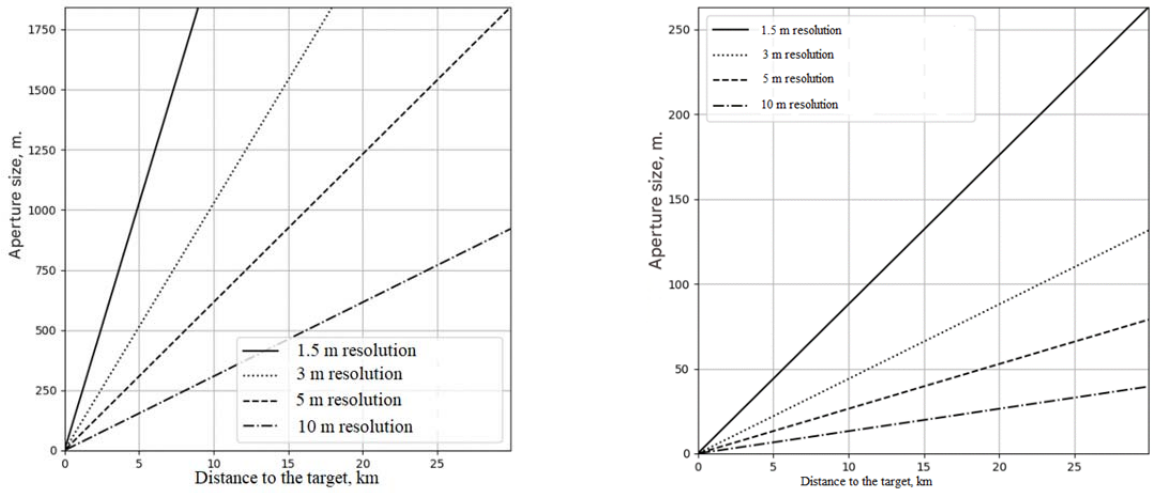

Fig. 3. Family of curves X_c from r_o for different δl: *a* – for $\lambda = 70$ cm, *b* – for $\lambda = 3$ cm

signal samples from each elementary reflector across the range strips [13]. For this, the following inequality must be satisfied in the synthesis interval $T_c = X_c/V_п$:

$$\Delta r_i(t) = r_i(t) - r_{0k} \leq \delta r, \qquad (8)$$

where r_{ok} is the traverse slant range to the k-th range strip; $\Delta r_i(t)$is the slant range increment to the i-th elementary reflector over the synthesis interval T_c. Given the equality $\delta r = \delta l$ we obtain the inequality:

$$r_{0k} \leq \frac{8\delta l^3}{\lambda^2}, \qquad (9)$$

from which it follows that signal migration across range channels for the accepted values begins at a slant range greater than 60 m (for the X-band, 30,000 m), i.e., in the P-band, it is almost always the same.

Fourth, random deviations in the trajectory signal phase lead to broadening of radar responses from point reflectors in radar images [6, 12]. This can lead both to distortion of images from distributed targets and to incorrect identification of small targets.

All of these difficulties are addressed in real-world systems by employing various compromises, such as mathematical compensation for range channel migration during signal processing, or the need to obtain and incorporate information from onboard micronavigation sensors to compensate for trajectory instabilities. All of this significantly complicates trajectory signal processing algorithms.

Structure of the side-looking SAR algorithmic support for radar image formation

Based on the information presented previously, the radar image formation algorithm can be generally represented as follows (fig. 4).

First, a radar signal is sent to the input, from which a radio hologram (RHG) of the received complex signal is prepared. Taking into account (5), it is advisable to perform range compression of the signal directly in the side-looking SAR. Compensation is provided for trajectory instabilities of the RHG and range channel migration. Next, a two-dimensional direct Fourier transform is performed to obtain the RHG spectrum. A direct Fourier transform of the two-dimensional support function is then performed to obtain the reference spectrum. The spectra of the support function and the RHG are multiplied. The support function is calculated for a given range to compensate for the phase of points at this range. A two-dimensional inverse Fourier transform of the

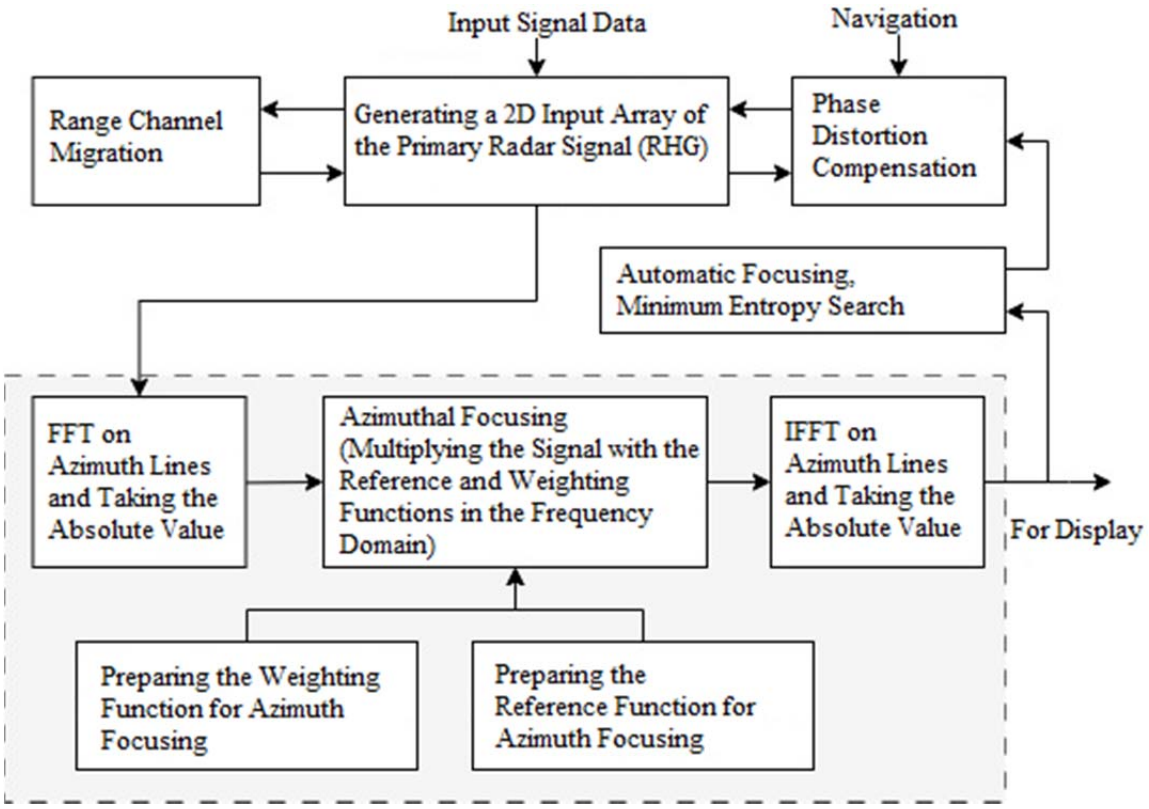

Fig. 4. Structural diagram of the radar image formation algorithm

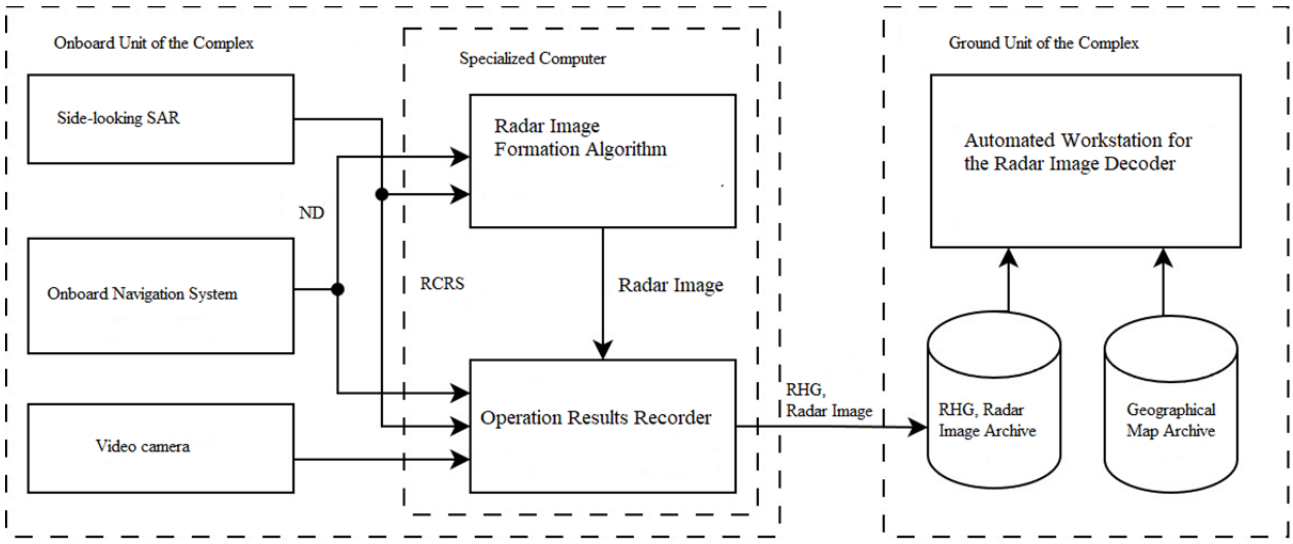

Fig. 5. Structural diagram of the airborne radar reconnaissance complex “Arkheolog-I”

multiplied spectra is performed to convert the data to the time domain. The result is the desired data – a radar image [14, 15].

Figure 5 shows the structural diagram of the airborne radar reconnaissance complex “Arkheolog-I”, developed on an initiative basis by the creative team of NaukaSoft Scientific and Production Association.

The onboard unit of the complex consists of a specialized computer, an onboard navigation system, and a side-looking P-band radar. Navigation definitions (ND) are used to compensate

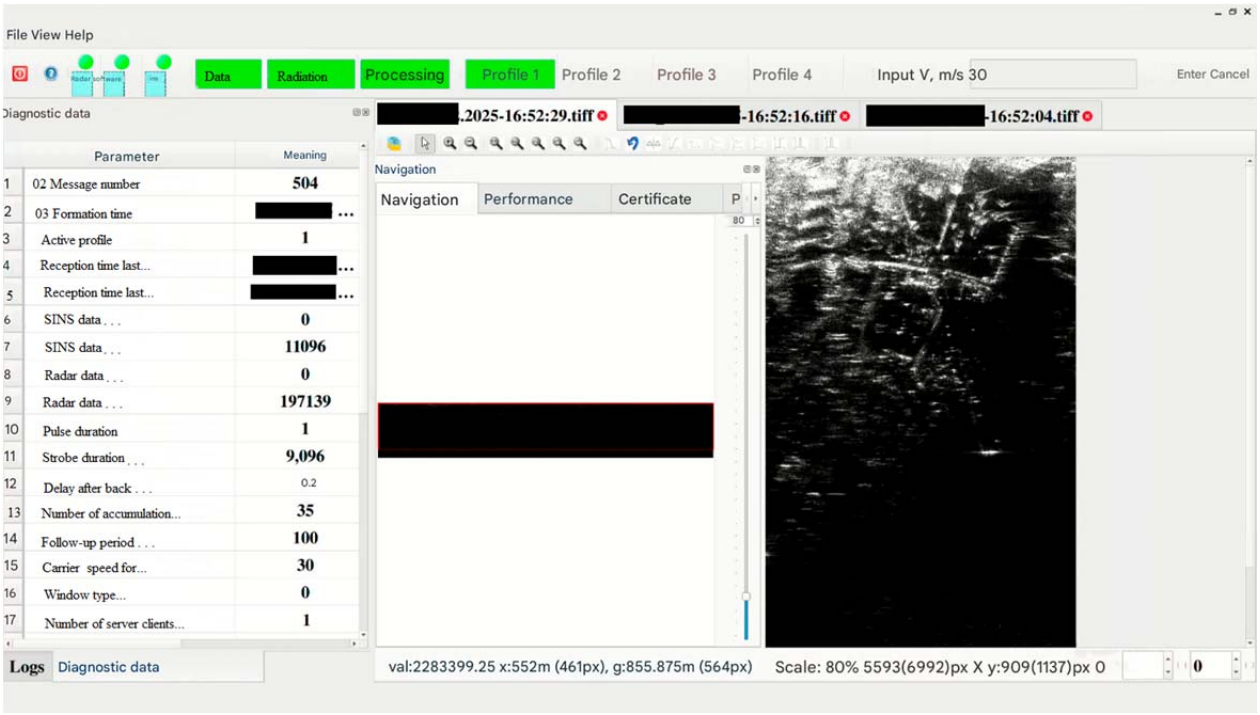

Fig. 6. Interface of the decoder operator's automated workstation

for trajectory instabilities in radar holograms, which consist of a range-compressed radio signal (RCRS). All system operation results, such as received RHG, ND, and received radar images, are stored in the specialized computer's internal memory.

The ground unit of the complex consists of a database containing archives of received RHG, radar images, and geographical maps. Geographical maps are used for georeferencing the received radar images to the terrain. Storing RHG for each radar image allows for repeated image acquisition operations with refined parameters, for example, for precise focusing of the radar image in a specific area of interest. The interface of the automated workstation (AWS) for the decoder operator for the airborne radar reconnaissance complex "Arkheolog-I" is shown in Figure 6.

The decoder operator's automated workstation performs the following tasks:

1. Receiving data from the Primary Processing Software (PDP) and display of radar images.
2. Receiving and displaying navigation data.
3. Preliminary processing of radar images.
4. Geometric correction and transformation of radar images.
5. Linking radar images to a digital terrain map [16].
6. Decoding radar images for detection, recognition, and determination of parameters of objects of interest [17].
7. Data archiving for repeated access.
8. Generating messages to users.

Experimental Observation Results

Experimental data describing the features of the use of the P-band SAR as part of an engineer reconnaissance system for humanitarian demining missions are presented below.

Figure 7, *a* shows the appearance of the airborne radar reconnaissance complex "Arkheolog-I", placed on a carrier – a medium-class UAV of the "Quadcopter" type, and Figure 7, *b* – airborne P-band radar "Linza".

On the radar of the P-band in shades of gray (fig. 8, *b*) and in the 3D representation (fig. 8, *c*), mine simulators (fig. 8, *a*) (three metal bowls up to 30 cm in diameter) and explosive reactive objects (two cuts of a metal water pipe 35 cm long)

a b

Fig. 7. *a* – airborne radar reconnaissance complex “Arkheolog”, *b* – airborne P-band radar “Linza”, dimensions 43×38×27 cm, weight up to 9 kg

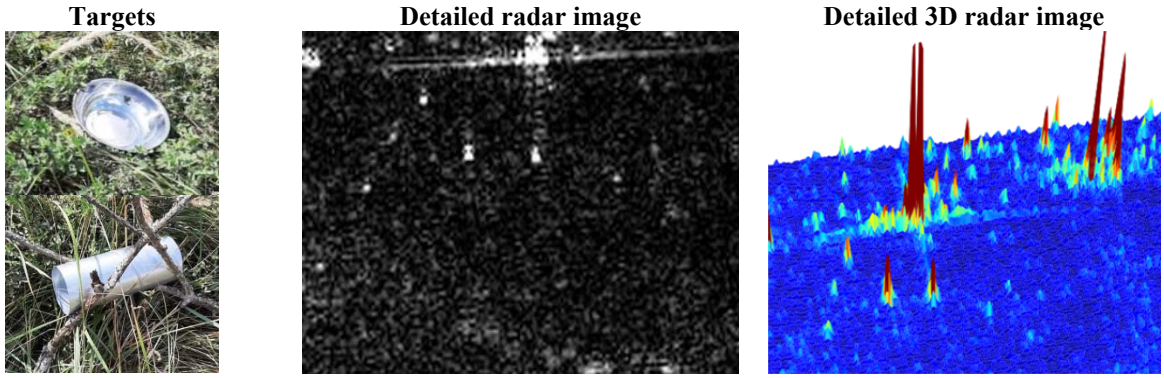

a b c

Fig. 8. Radar image of dry steppe in summer with mine simulators

a b

Fig. 9. Flight experiment using a VTOL UAV

are observed. The carrier’s flight altitude was up to 300 m, and the slant range to the objects was less than 600 m. Despite the relative uniformity of the underlying surface, the radar image shows spots resulting from the random summation of reflected signals from elementary surface areas, a phenomenon known as “speckle” patterns.

Figure 9, *a* shows a variant of mounting the onboard radar reconnaissance complex on a VTOL UAV. The flight mission involved flying along a rectangular perimeter at an altitude of up to 300 m, a speed of up to 100 km/h, and an inclined distance of up to 400 m from the target installation center. A strong crosswind (up to

Fig. 10. Targets and their placement diagram

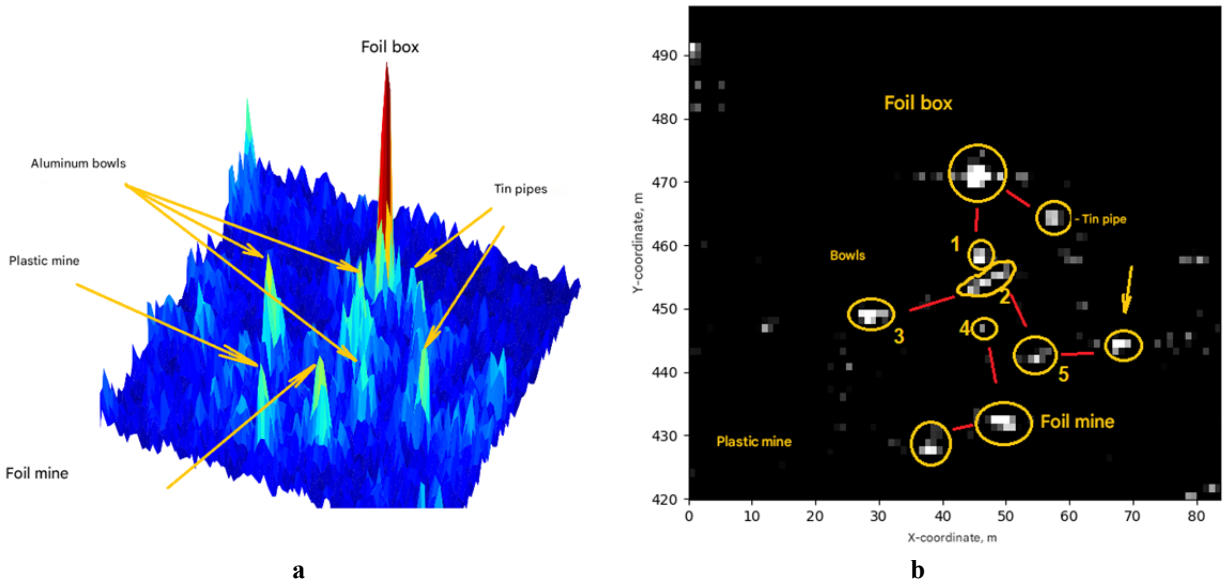

Fig. 11. Radar images of targets on a humid steppe background during spring

15 m/s) adjusted the route, significantly altering the carrier's flight trajectory, as can be seen in Figure 9, *b*. Targets in the form of bowls, pipe cuts, and TM-62 plastic training anti-tank mines (fig. 10, *a*) were placed every 10 m, as shown in Figure 10, *b*.

Figure 11 shows 3D (fig. 11, *a*) and 2D (fig. 11, *b*) radar images of a surface area with targets.

Despite the significant trajectory curvature, processing was able to focus the reflected signals and obtain significant radar contrast. Radar image interpretation allowed detection and identification of 10 of the 12 targets (fig. 11, *b*). The maximum amplitude was observed in the signal reflected from the foil-wrapped cardboard box. The interpretation process was complicated by the relative shift in the maximum reflections from the targets, caused by the significant deviation in the carrier's flight path.

Conclusion

The conducted flight experiments demonstrated the high information content of the P-band SAR system for engineer reconnaissance missions. A VTOL UAV, with its greater longitudinal flight stability, appears to be the preferred carrier. Thus, the task of providing infor-

mation support for humanitarian demining can be accomplished through the integrated use of UAVs with various payloads in several stages.

At the first stage, an orthophoto map of the area intended for demining is created using TV cameras and laser locators. Then, radar and IR images are generated, combined processing, after overlaying the orthophoto map, will allow for the construction of a minefield cadastral register. This information can be refined by an additional UAV flight with a minefield payload. This will ensure a consistent increase in the detail, completeness, and reliability of the information: "no mines" – "mines localized in the specified areas" – "cadastral register of the minefield with mine coordinates."

The need to process large volumes of complex information requires maximum automation of the image decoder operator. This requires the use of artificial intelligence technologies, which require large volumes of training samples and significant computing resources.

References

1. Severov, N.V. (2003). Application of robotics in emergency situations: theory and practice: Monograph. Novogorsk: AGZ MCHS Rossii, 241 p. (in Russian)

2. Petrenko, E.S. (2024). Some technical features of the solution to the problem of humanitarian demining. Systems of technical protection of objects. *vrsystems.ru*. Available at: https://www.vrsystems.ru/stati/nekotorie_texnicheskie_osobennosti_resheniya_problemi_gumanitarnogo_razminirovaniya.htm (accessed: 21.04.2025). (in Russian)

3. Baur, J. (2024). Ukraine is riddled with land mines: drones and ai can help. *IEEE Spectrum*, vol. 61, no. 5, pp. 42–49. DOI: 10.1109/MSPEC.2024.10522930

4. Gorshkov, P.S, Vasiliev, O.V. (2024). New technical means of reconnaissance in the interests of humanitarian demining. *In: Innovatsionnyye, informatsionnyye i kommunikatsionnyye tekhnologii: sbornik trudov XXI Mezhdunarodnoy nauchno-prakticheskoy konferentsii*. Moscow: Assotsiatsiya vypusknikov i sotrudnikov VVIA im. prof. N.Ye. Zhukovskogo, pp. 131–135. (in Russian)

5. Shkolnyy, LA., Tolstov, E.F., Detkov, A.N. et al. (2008). Onboard radar reconnaissance systems and decoding of radar images: Tutorial, in Shkolnyy LA. (Ed.). Moscow: Izdatelstvo VVIA im. prof. N.Ye. Zhukovskogo, 432 p. (in Russian)

6. Kondratenkov, G.S., Frolov, A.Yu. (2005). Radiovision. Spaceborne Radar Earth-Observation Stations: textbook for universities, in Kondratenkov G.S. (Ed.). Moscow: Radiotekhnika, 368 p. (in Russian)

7. Tolstov, E.F., Filonchikov, V.D., Shkolnyy, L.A. (1993). Radio engineering circuits and signals. Theory of signals, linear circuits and systems. Moscow: Izdatelstvo VVIA im. prof. N.Ye. Zhukovskogo, 720 p. (in Russian)

8. Tihonov, V.I., Harisov, V.N. (1989). Theory, Methods of Analysis and Synthesis of Radio-Electronic Systems. Moscow: Izdatelstvo VVIA im. prof. N.Ye. Zhukovskogo, 609 p. (in Russian)

9. Kondratenkov, G.S., Hotlyannik, V.A., Ivanisov, B.A. (2000). Statistical Characteristics of Signals of Decimeter Band Synthetic Aperture Radar Stations. *Radiotekhnika*, no. 3, pp. 55–60. (in Russian)

10. Vasilyev, O.V., Detkov, A.N., Zinchenko, O.N., Krishtopov, A.V., Tsvetkov, O.E. (2016). The compact p-band UAV'S SAR. *Information-measuring and control systems*, vol. 14, no. 2, pp. 44–54. (in Russian)

11. Vasilyev, O.V., Detkov, A.N. (2018). Small-sized integrated two-band SAR for a UAV of monitoring of an ice surface in the arctic region. *Polet*, no. 7, pp. 17–23. (in Russian)

12. Neronskiy, L.B., Mikhaylov, V.F., Bragin, I.V. (1999). Microwave equipment for remote sensing of the Earth's surface and atmosphere. Radars with synthetic aperture antennas: Tutorial. Part 2. St. Petersburg: SPbGUAP, 220 p. (in Russian)

13. Shkolnyy, L.A. (1981). Two ways to describe the operator's sensing during the syn-

thesizing of the RSA signal processing system by coordinate path range. *In: NMM po impul'snoy tekhnike i sadovoy obrabotke informatsii: sbornik statey*. Moscow: Izdatelstvo VVIA im. prof. N.Ye. Zhukovskogo, pp. 112–119. (in Russian)

14. Cumming, I., Wong, F. (2005). Digital processing of synthetic aperture radar data: algorithms and implementation. Artech House Publishers, 625 p.

15. Fang, J., Xu, Z., Zhang, B., Hong, W., Wu, Y. (2014). Fast compressed sensing SAR imaging based on approximated observation. *IEEE Journal of Selected Topics in Applied Earth Observations and Remote Sensing*, vol. 7, no. 1, pp. 352–363. DOI: 10.1109/JSTARS.2013.2263309

16. Tonkih, A.N., Kuznetsova, V.A. (2023). Automated georeferencing of sar images using machine vision methods. *In: Aktualnyye problemy i perspektivy razvitiya radiotekhnicheskikh i infokommunikatsionnykh sistem ("RADIOINFOKOM-2023"): sbornik nauchnykh statey VII Mezhdunarodnoy nauchno-prakticheskoy konferentsii*. Moscow: MIREA, pp. 38–42. (in Russian)

17. Vlasov, S.O., Glasyshev, A.I., Boguslavsky, A.A., Sokolov, S.M. (2023). Example of the object detection problem solving using neural network technologies. *Preprinty IPM im. M.V. Keldysha*, no. 16, 27 p. DOI: 10.20948/prepr-2023-16 (in Russian)

Список литературы

1. Северов Н.В. Применение робототехники в чрезвычайных ситуациях: теория и практика: монография. Новогорск: АГЗ МЧС России, 2003. 241 с.

2. Петренко Е.С. Некоторые технические особенности решения проблемы гуманитарного разминирования. Системы технической охраны объектов [Электронный ресурс] // vrsystems.ru. URL: https://www.vrsystems.ru/stati/nekotorie_texnicheskie_osobennosti_resheniya_problemi_gumanitarnogo_razminirovaniya.htm (дата обращения: 21.04.2025).

3. Baur J. Ukraine is riddled with land mines: drones and ai can help // IEEE Spectrum. 2024. Vol. 61, no. 5. Pp. 42–49. DOI 10.1109/MSPEC.2024.10522930

4. Горшков П.С., Васильев О.В. Новые технические средства разведки в интересах гуманитарного разминирования // Инновационные, информационные и коммуникационные технологии: сборник трудов XXI Международной научно-практической конференции. Сочи, 01-10 октября 2024 г. Москва: Ассоциация выпускников и сотрудников ВВИА им. проф. Жуковского, 2024. С. 131–135.

5. Школьный Л.А., Толстов Е.Ф., Детков А.Н. и др. Радиолокационные системы воздушной разведки, дешифрирование радиолокационных изображений: учеб. пособие / Под. ред. Л.А. Школьного. М.: Изд-во ВВИА им. проф. Н.Е. Жуковского, 2008. 432 с.

6. Кондратенков Г.С., Фролов А.Ю. Радиовидение. Радиолокационные станции дистанционного зондирования Земли: учеб. пособие для вузов / Под ред. Г.С. Кондратенкова. М.: Радиотехника, 2005. 368 с.

7. Толстов Е.Ф., Филончиков В.Д., Школьный Л.А. Радиотехнические цепи и сигналы. Теория сигналов, линейных цепей и систем. М.: Изд-во ВВИА им. проф. Н.Е. Жуковского, 1993. 720 с.

8. Тихонов В.И., Харисов В.Н. Теория, методы анализа и синтеза радиоэлектронных систем. М.: Изд-во ВВИА им. проф. Н.Е. Жуковского, 1989. 609 с.

9. Кондратенков Г.С., Хотлянник В.А., Иванисов Б.А. Статистические характеристики сигналов РЛС с синтезированной апертурой дециметрового диапазона // Радиотехника. 2000. № 3. С. 55–60.

10. Васильев О.В. Малогабаритная радиолокационная система Р-диапазона беспилотных летательных аппаратов / О.В. Васильев, А.Н. Детков, О.Н. Зинченко, А.В. Криштопов, О.В. Цветков // Информационно-измерительные

ные и управляющие системы. 2016. Т. 14, № 2. С. 44–54.

11. Васильев О.В., Детков А.Н. Малогабаритная двухдиапазонная радиолокационная станция с синтезированной и интегрированной апертурой антенны для беспилотного летательного аппарата воздушной ледовой разведки в арктическом регионе // Полет. Общероссийский научно-технический журнал. 2018. № 7. С. 17–23.

12. Неронский Л.Б., Михайлов В.Ф., Брагин И.В. Микроволновая аппаратура дистанционного зондирования поверхности Земли и атмосферы. Радиолокаторы с синтезированной апертурой антенны: учеб. пособие. СПб.: СПбГУАП, 1999. Ч. 2. 220 с.

13. Школьный Л.А. Два способа описания оператора зондирования при синтезе системы обработки сигналов в РСА по координате путевая дальность // НММ по импульсной технике и дискретной обработке информации: сборник статей. М.: Изд-во ВВИА им. проф. Н.Е. Жуковского, 1981. С. 112–119.

14. Cumming I., Wong F. Digital processing of synthetic aperture radar data: algorithms and implementation. Artech House Publishers, 2005. 625 p.

15. Fang J. Fast compressed sensing SAR imaging based on approximated observation / J. Fang, Z. Xu, B. Zhang, W. Hong, Y. Wu // IEEE Journal of Selected Topics in Applied Earth Observations and Remote Sensing. 2014. Vol. 7, no. 1. Pp. 352–363. DOI: 10.1109/JSTARS.2013.2263309

16. Тонких А.Н., Кузнецова В.А. Автоматизированная геопривязка радиолокационных изображений с применением методов машинного зрения // Актуальные проблемы и перспективы развития радиотехнических и инфокоммуникационных систем («РАДИОИНФОКОМ-2023»): сборник научных статей VII Международной научно-практической конференции. Москва, 20–24 ноября, 2023 г. М.: МИРЭА, 2023. С. 38–42.

17. Власов С.О. Решение задачи обнаружения объекта с помощью нейросетевых технологий / С.О. Власов, А.И. Гладышев, А.А. Богуславский, С.М. Соколов // Препринты ИПМ им. М.В. Келдыша. 2023. № 16. 27 с. DOI: 10.20948/prepr-2023-16

Information about the authors

Oleg V. Vasiliev, Doctor of Technical Sciences, Professor, Principal Researcher, NaukaSoft Scientific and Production Association, vas_ov@mail.ru.

Pavel S. Gorshkov, Doctor of Technical Sciences, General Director of NaukaSoft Scientific and Production Association, vas_ov@mail.ru.

Sergey A. Zyabkin, Candidate of Technical Sciences, Research Associate, NaukaSoft Scientific and Production Association, sergezyab@gmail.com.

Sergey P. Shepet', Candidate of Technical Sciences, Professor, Professor of the Technological Institute of Service (branch of the Don State Technical University), ship.1963@mail.ru.

Сведения об авторах

Васильев Олег Валерьевич, доктор технических наук, профессор, главный научный сотрудник ООО «НПО НаукаСофт», vas_ov@mail.ru.

Горшков Павел Сергеевич, доктор технических наук, доцент, генеральный директор ООО «НПО НаукаСофт», vas_ov@mail.ru.

Зябкин Сергей Алексеевич, кандидат технических наук, научный сотрудник ООО «НПО НаукаСофт», sergezyab@gmail.com.

Шепеть Сергей Петрович, кандидат технических наук, профессор, профессор Технологического института сервиса (филиал Донского ГТУ), ship.1963@mail.ru.

Поступила в редакцию	08.07.2025	Received	08.07.2025
Одобрена после рецензирования	25.08.2025	Approved after reviewing	25.08.2025
Принята в печать	22.01.2026	Accepted for publication	22.01.2026